Catalysis Letters Vol. 84, Nos. 3–4, December 2002 (©2002)

A comparative study of the N_2O–CO and N_2O–H_2 reactions on the Ir(110) surface with emphasis on the oscillatory behavior

Sónia A.C. Carabineiro [a], Wibo D. van Noort [b], and Bernard E. Nieuwenhuys [a,*]

[a] *Leiden University, Leiden Institute of Chemistry, Surface Science and Heterogeneous Catalysis Group, Einsteinweg 55,*
P.O. Box 9502, 2300 RA Leiden, The Netherlands
[b] *Philips Research Leuven, Kapeldreef 75, B-3001 Leuven, Belgium*

Received 15 July 2002; accepted 13 September 2002

The N_2O–CO reaction has been studied on the Ir(110) surface in the temperature range from 300 up to 800 K and compared with the N_2O–H_2 reaction on the same surface. At temperatures up to 550 K (depending on the N_2O/reducing gas ratio), the reaction with H_2 is faster due to CO inhibition of the reduction of N_2O by CO. Isothermal sustained oscillations in rate were found in the temperature range from 373 to 377 K, for very low CO/N_2O ratios. The reaction products are N_2 and CO_2. Interestingly, the reactant N_2O oscillates in an almost counter-phase with the other reactant, CO. The period is around 60 s; also, highly correlated, synchronous events were found in regular time intervals. A model for the rate oscillations involves periodic transitions between a CO-rich (inactive) and a CO-poor (active) surface. In contrast, the rate oscillations for the N_2O–H_2 reaction are related to periodic transitions between O-rich and O-poor surfaces.

KEY WORDS: oscillations; nitrogen oxides; nitrogen molecule; carbon monoxide; catalysis; chemisorption; surface chemical reaction; iridium.

1. Introduction

Nitrous oxide is an important greenhouse gas and it participates in cyclic reactions that lead to ozone destruction [1–4]. As a continuation of our earlier research on NO adsorption and reaction, we started a project focused on a better understanding of the N_2O–metal interaction. In this project the adsorption and reactions of N_2O are studied on various noble metal surfaces. A previous paper dealt with the N_2O–H_2 reaction on the Ir(110) surface [5]. Both the N_2O–CO and N_2O–H_2 reactions are of importance in automotive catalytic converters, since N_2O is a side or intermediate product in NO reduction [6–10]. The N_2O that is formed can undergo further reaction with CO, H_2 or hydrocarbons to produce the desired products: N_2, CO_2, and H_2O. With CO, NO reduction may involve three reactions [6,8,9]:

$$CO + NO \rightarrow \tfrac{1}{2}N_2 + CO_2 \qquad (1)$$

$$CO + 2NO \rightarrow N_2O + CO_2 \qquad (2)$$

$$CO + N_2O \rightarrow N_2 + CO_2. \qquad (3)$$

Reactions (1) and (2) are the most well studied, and a number of studies have been published on the N_2O–CO reaction, mainly on Pt, Pd, and Rh supported on alumina [6–10]. Sadhankar *et al.* described a model for the reaction on alumina-supported Pt that incorporates the $(1 \times 1) \leftrightarrow$ hex surface phase transformation of Pt(100) [7,9]. The model is based on a reaction mechanism consisting of three elementary steps, namely, the reversible adsorption of CO, the irreversible dissociative adsorption of N_2O to form adsorbed oxygen and gaseous N_2, and the reaction of adsorbed carbon monoxide and adsorbed atomic oxygen to produce gaseous CO_2.

To the best of our knowledge no work has been reported before for the N_2O–CO reaction on Ir surfaces. In the present paper the reduction of N_2O by CO on the Ir(110) surface will be compared to that by H_2. Previous papers dealt already with the adsorption of N_2O [5], H_2 and CO [11] on this same surface.

2. Experimental

Experiments were performed in an ultra-high vacuum (UHV) system equipped with facilities for LEED, AES, and a differentially pumped quadrupole mass spectrometer. The system was pumped by a turbo molecular pump and an ion pump. The base pressure was always better than 2×10^{-10} mbar. The gases were dosed by means of three leak valves from the dosing system into the main chamber.

The Ir sample was cut from an Ir single crystal by spark erosion to within 0.5° of the desired direction and polished down to a grain size of 1 μm. The crystal was spotwelded to a Ta support and could be heated resistively up to 1400 K. The temperature was measured using a Pt–Pt/Rh thermocouple, which was spotwelded

---

[*] To whom correspondence should be addressed.
E-mail: b.nieuwe@chem.leidenuniv.nl

to the back of the crystal. The crystal was cleaned by multiple heating cycles in an oxygen or hydrogen atmosphere, Ar^+ ion bombardment, and flashing in UHV to 1400 K. The Ar^+ ion sputtering and flashing treatments were repeated at the beginning of each series of experiments and the surface cleanliness and structure were checked by AES and LEED.

During the reactions, the crystal was turned in front of a small opening which gave access to the quadrupole mass spectrometer (QMS) chamber. Reactions were performed in the flow mode using a turbomolecular pump.

High-purity gases (Messer Griesheim, purity 99.5–99.999%) were used without further purification. The pressure readings of the ion gauge were corrected using relative sensitivities for N_2O and CO to N_2 of 1.0 and 1.05, respectively. Since some species have the same mass (CO and N_2, mass 28; N_2O and CO_2, mass 44), the use of labeled CO (^{13}CO from Sigma Aldrich) was required to distinguish them. To make reading easier it will be further referred to in the text simply as CO.

Further details of experimental procedures are described elsewhere [5].

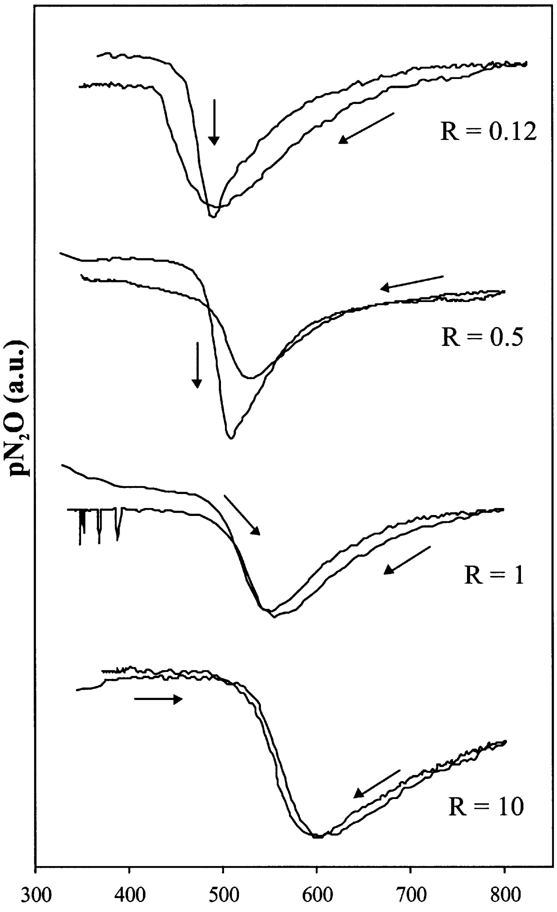

Figure 1. Heating and cooling cycles performed in a flow of 1×10^{-6} mbar N_2O, for several CO/N_2O ratios (R), at a heating rate of 20 K/min. Change in pressure of mass 44 (N_2O) is shown. The maximum conversion of N_2O varied from 25% (for $R = 0.12$) to 13% ($R = 10$).

3. Results and discussion

3.1. Heating and cooling cycles

Heating and cooling cycles from 300 to 800 K performed in a flow of N_2O at a pressure of 1×10^{-6} mbar, in the absence and presence of CO, showed that in the former case there was almost no decomposition of N_2O in the steady state. In the presence of CO, evidence of reaction was found in the temperature range between 450 and 700 K, as shown in figure 1. The higher the ratio CO/N_2O, the higher the temperature at which the reaction starts. For example, at $R = 0.25$, N_2O reaction starts at 450 K and for $R = 10$, temperatures higher than 500 K are needed for N_2O reduction.

For comparison, figure 2 shows similar experiments performed for the N_2O–H_2 reaction. Increasing the H_2/N_2O ratio above the stoichiometric ratio of 1 did not enhance the reaction rate significantly [5]. The N_2O–H_2 reaction starts at much lower temperature than the N_2O–CO reaction. For example, for a reductant/N_2O ratio (R) of unity, at 470 K, the N_2O conversion is almost zero when CO is used as a reducing gas and it is around 50% of its maximum value when

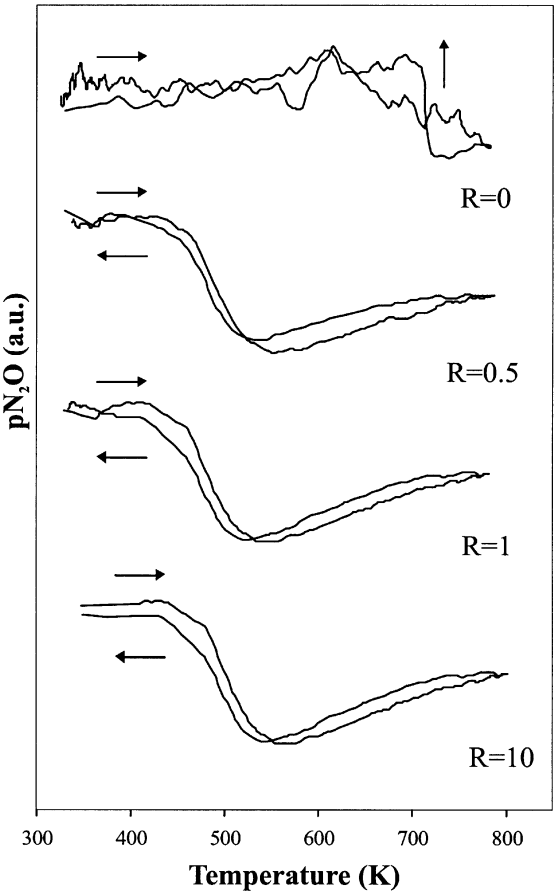

Figure 2. Heating and cooling cycles performed in a flow of 1×10^{-6} mbar N_2O, for several H_2/N_2O ratios (R), at a heating rate of 20 K/min. Change in pressure of mass 44 (N_2O) is shown. The maximum conversion of N_2O varied from 4% ($R = 0$) to 20% ($R = 10$).

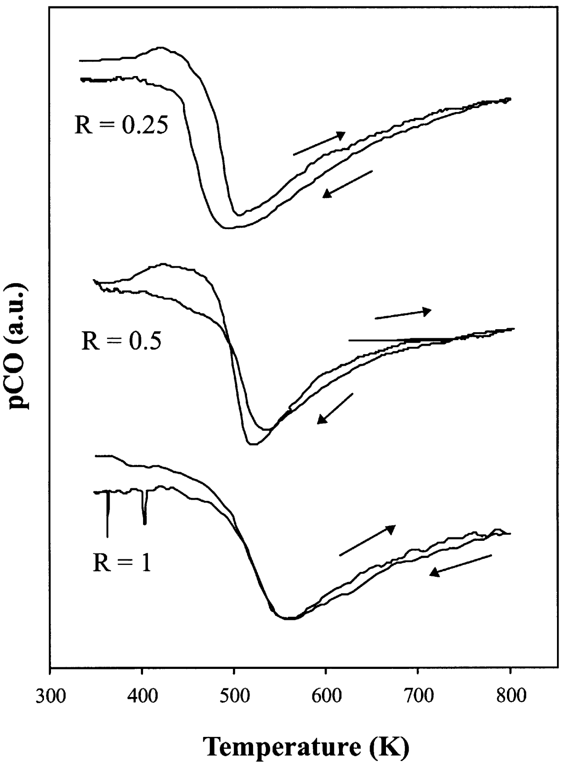

Figure 3. Heating and cooling cycles performed in a flow of 1×10^{-6} mbar N_2O, for several CO/N_2O ratios (*R*), at a heating rate of 20 K/min. Change in pressure for mass 29 (^{13}CO) is shown.

hydrogen is used. For higher values of *R*, the differences are much larger. For $R = 10$, around 525 K, the N_2O conversion is still almost zero with CO, and with H_2 it is close to its maximal value.

Figure 3 also shows that the higher the ratio, the higher the temperature at which CO starts to be converted. Figure 4 shows a typical example of the N_2 evolution during heating and cooling cycles performed for the N_2O–CO reaction. There is a sharp increase of the N_2 pressure when the reaction starts to take place. The same is observed for the CO_2 evolution (figure 5). The higher the CO/N_2O ratio the higher the temperature at which the products start to be formed and the higher the conversion in the higher temperature range (~700 K).

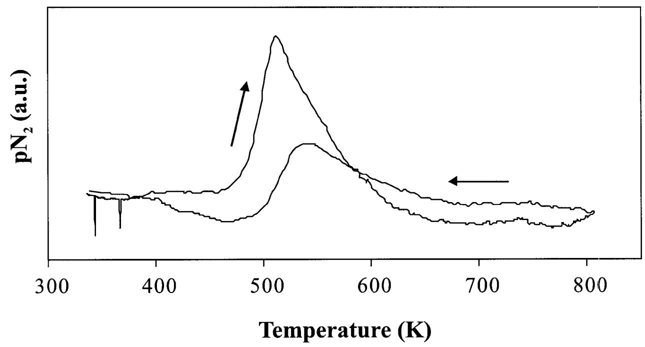

Figure 4. Heating and cooling cycle performed in a flow of 1×10^{-6} mbar N_2O, for a CO/N_2O ratio of 0.5, at a heating rate of 20 K/min. Change in pressure for mass 28 (N_2) is shown.

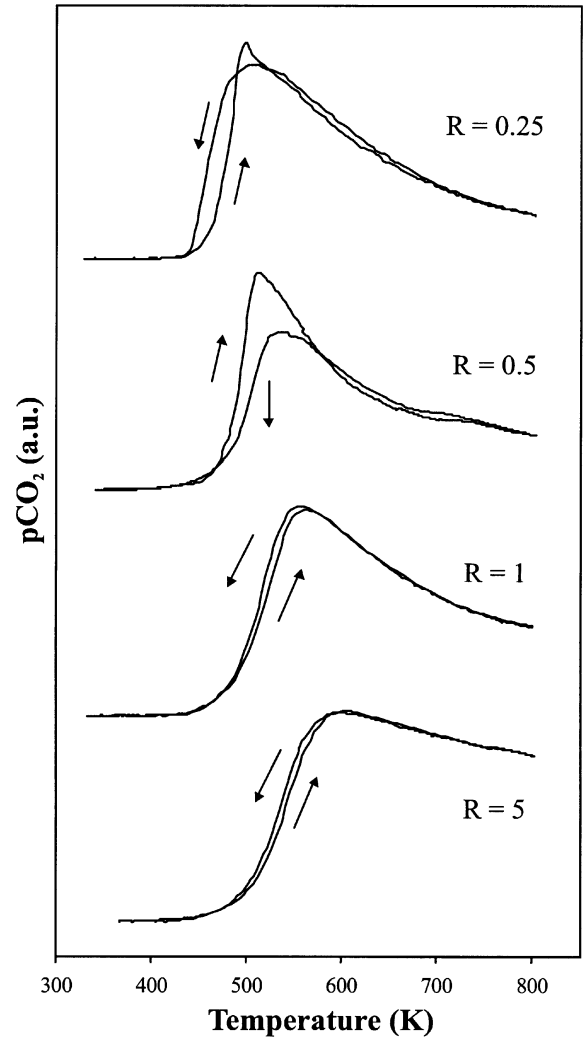

Figure 5. Heating and cooling cycles performed in a flow of 1×10^{-6} mbar N_2O, for several CO/N_2O ratios (*R*), at a heating rate of 20 K/min. Change in pressure for mass 45 ($^{13}CO_2$) is shown.

N_2 and CO_2 are the only products found. Hence, the results can be interpreted in terms of the following mechanism, also proposed by other authors [7,9]:

$$N_2O_{(g)} \rightarrow N_{2(g)} + O_{ads} \tag{4}$$

$$CO_{(g)} \rightarrow CO_{ads} \tag{5}$$

$$CO_{ads} + O_{ads} \rightarrow CO_{2(g)} \tag{6}$$

Step (1) is accepted by several authors, since it is agreed that while oxygen remains adsorbed on the surfaces, N_2 desorbs [5,18–20].

The effect of the CO/N_2O ratios on the temperature at which the reaction starts and the fact that the reaction with H_2, in the temperature range 450–500 K, is faster for similar reductant gas/N_2O ratios, suggest that CO inhibits the reaction when present in higher concentrations. This observation is in agreement with results

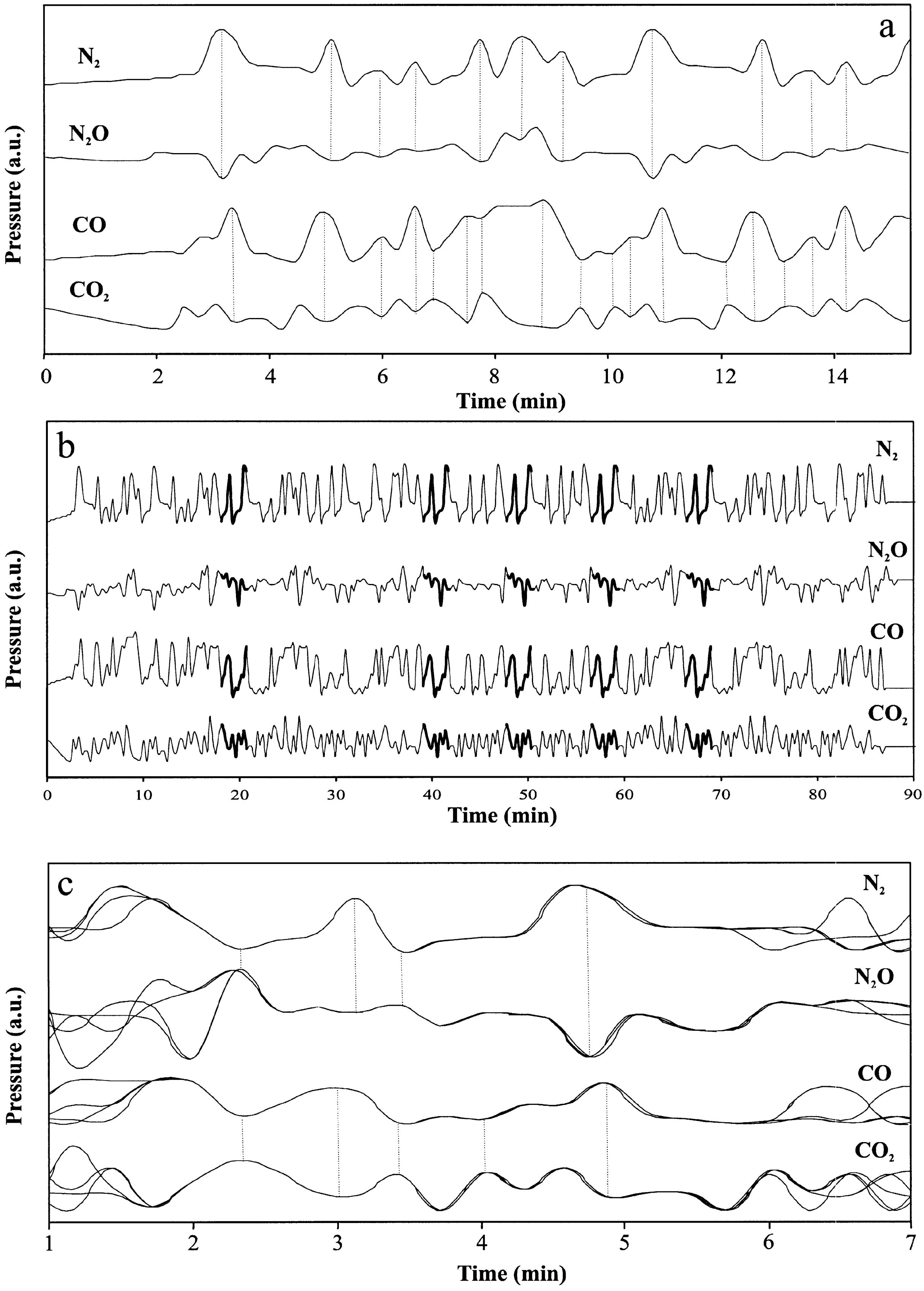

Figure 6. Oscillations in the partial pressures of N_2O, N_2, CO, and CO_2, on the Ir(110) surface, at an N_2O pressure of 1×10^{-6} mbar. The temperature was kept constant at 373 K and the CO/N_2O ratio was 0.15. Graph (a) shows the first 15 min of oscillations. Graph (b) shows the entire time series with the repeating patterns highlighted. These are superimposed in graph (c).

reported for the N_2O–CO reaction over Rh catalysts [6]. McCabe and Wong [6] reported for the reaction over Rh, a reaction order of -1 in CO and $+0.65$ in N_2O at temperatures between 564 and 583 K. AES experiments carried out during heating and cooling cycles show the presence of CO on the surface until around 500 K. No build-up of other (N or O) species was observed. CO inhibition at low temperatures is well documented for the reaction of O_2-CO on Pt, Pd and Ir surfaces [12–15]. In the higher temperature range ($\sim$700 K) high CO pressures favor the N_2O conversion. This observation suggests that it is the CO concentration on the surface that determines the reaction rate and not the N_2O decomposition to O_{ads} and N_2 (step (4)).

Some instabilities can be observed in the N_2O pressure between 370 and 400 K (figures 1, 3, 4), which were thought to be related with the onset of rate oscillations in that temperature range. It was reported before that similar irregularities in rate during heating and cooling cycles can be linked to the onset of oscillations for the NO–H_2 [16,17] and N_2O–H_2 [5] reactions.

3.2. Oscillations in rate

In the temperature range between 373 and 377 K, sustained oscillations in rate were observed at an N_2O pressure of the order of 1×10^{-6} mbar, using very low CO/N_2O ratios (close to 0.1) as shown in figures 6 and 7. The oscillations were triggered by slowly heating the crystal in the presence of N_2O (1×10^{-6} mbar) with a very low amount of CO added, the smallest possible to be read by the ion gauge (resulting in a CO/N_2O ratio of approximately 0.05), from room temperature to 800 K and then subsequent cooling down to a temperature between 370 and 390 K (the range where irregularities in the rate of the reaction were detected for the heating and cooling cycles as shown in figures 1, 3, 4). Then the pressure of CO was increased stepwise until sustained oscillations in rate started.

Figures 6 and 7 show the oscillations at 373 and 375 K, respectively. The reaction products were N_2 and CO_2 as expected. The period of oscillations is approximately 60 s, just as in rate oscillations reported for the N_2O–H_2 reaction on the same surface [5]. As expected, the rate of N_2 formation oscillates in counter-phase with that of the reactant N_2O. Compared to the N_2O pressure, CO_2 was formed in low amounts because the relative pressure of CO was very low. CO_2 pressure oscillates in counter-phase with that of CO. Figures 6(a) and 7(a) show the oscillations in closer detail (the first 15 min). Figures 6(b) and 7(b) show the entire time series where oscillations were found at 373 and 375 K, respectively. The highlighted parts are highly correlated in time with an autocorrelation greater than 99%. These repeating patterns occur at exactly the same time for all observed masses, hence they are synchronous as figures 6(b) and 7(b) show. These repeating patterns are superimposed in figures 6(c) and 7(c), thus showing the in-phase and counter-phase relationships. It is shown that the time frames themselves are spaced in regular time intervals (as shown in the figures). This confirms the periodic nature of the patterns and the signal itself. The signal of each mass in the superimposed patterns has a distinctly different shape. Hence, a linear relationship (*e.g.*, the correlation function) is not sufficient to describe the relation between the observed masses. Note that the pressure of the reactant N_2O oscillates in an almost counter-phase with that of the other reactant CO. These repeating patterns were also observed in the N_2O–H_2 reaction.

AES measurements were also carried out during the rate oscillations, as was done with the N_2O–H_2 experiments [5]. For that purpose, the rate oscillations were started and the crystal was moved from the MS opening to the CMA opening. Measurement of a full AES spectrum takes about 2.5 min, which is insufficient to follow the evolution of the C/CO_{ads} peak intensity (around 272 eV) during one oscillation cycle (of 1 min). However, by monitoring the spectra during the oscillations, it was found that the O-coverage remains low during the oscillations and that the CO-concentration varies between a minimum and a maximum value with the rate oscillations. Hence, a clear relationship between the CO surface coverage and the oscillatory behavior is established, which is shown figure 8, where the $CO_{272\,eV}$/$Ir_{54\,eV}$ intensity *versus* time is plotted. This demonstrates that there are periodic transitions between a CO-rich (inactive) and a CO-poor (active) surface during the oscillations. The specific form of an oscillation cycle for the N_2O–CO reaction, as illustrated in figure 9, is used to propose some relevant steps in the oscillation mechanism:

1. The CO coverage becomes low, the surface is in its active state, the rate of N_2O conversion is high, and the removal of O_{ads} by CO_{ads} (step (6)) is slower than its formation (step (4)).
2. N_2O decomposition is maximal and CO is efficiently removed by O_{ads}.
3. CO adsorption becomes faster than its removal by O_{ads}. As a result, CO build-up starts and it also inhibits reaction (4), so the N_2O conversion drops.
4. O_{ads} is efficiently removed by CO_{ads} to CO_2. The rate of CO_2 production and the rate of CO adsorption are maximum. The N_2O conversion and the O_{ads} concentration are low.

For the N_2O–H_2 reaction, AES measurements showed that the O-concentration varied from zero to a maximum value during the rate oscillations. Also "oscillatory" behavior was found in the plot of the $O_{510\,eV}$/$Ir_{54\,eV}$ intensity *versus* time [5]. A build-up of atomic oxygen on the crystal surface, produced by N_2O decomposition, would result in a decrease in the rate of N_2O dissociation, until oxygen is released in the

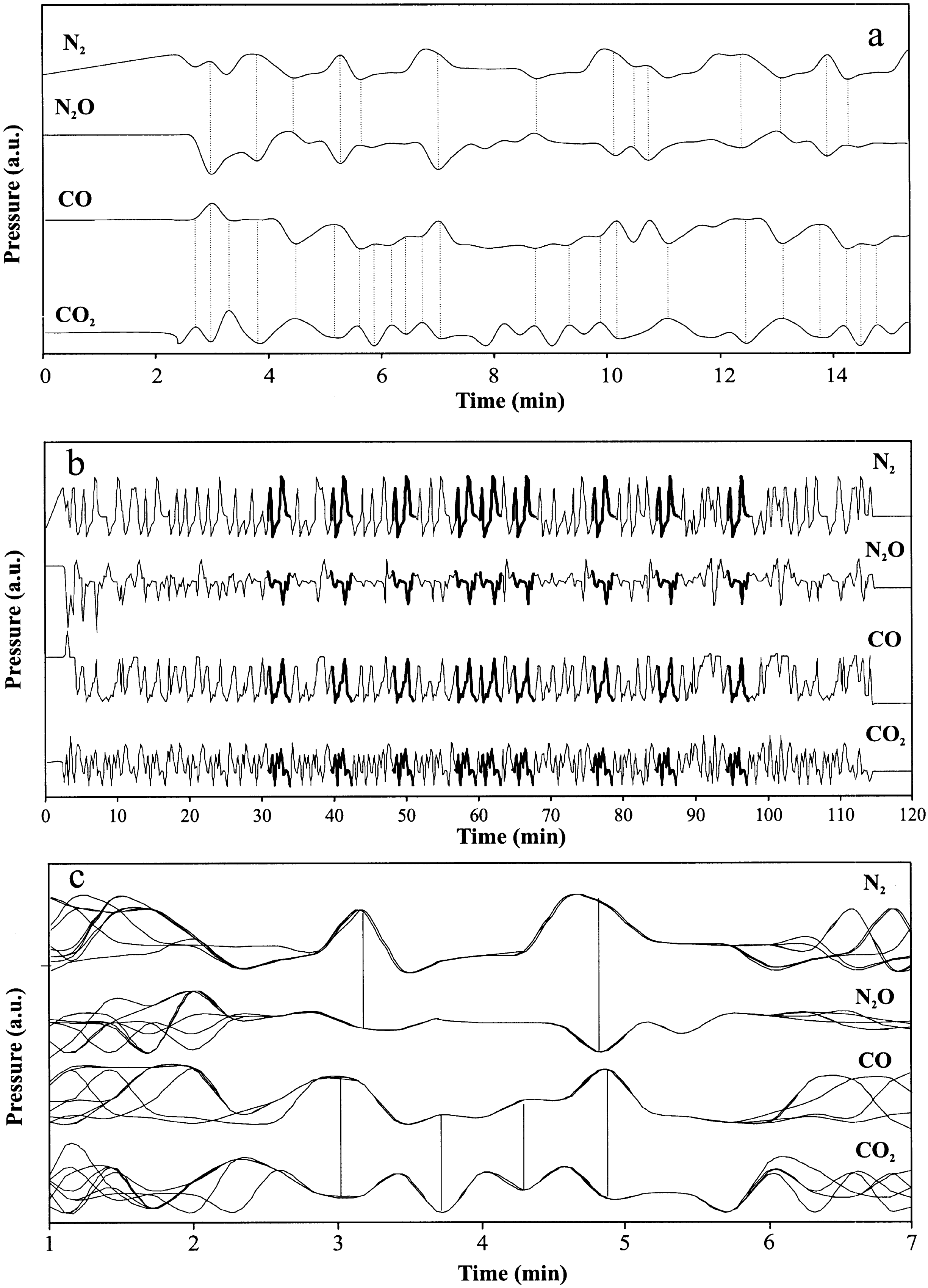

Figure 7. Oscillations in the partial pressures of N_2O, N_2, CO, and CO_2, on the Ir(110) surface, at an N_2O pressure of 1×10^{-6} mbar. The temperature was kept constant at 375 K and the CO/N_2O ratio was 0.1. Graph (a) shows the first 15 min of oscillations. Graph (b) shows the entire time series with the repeating patterns highlighted. These are superimposed in graph (c).

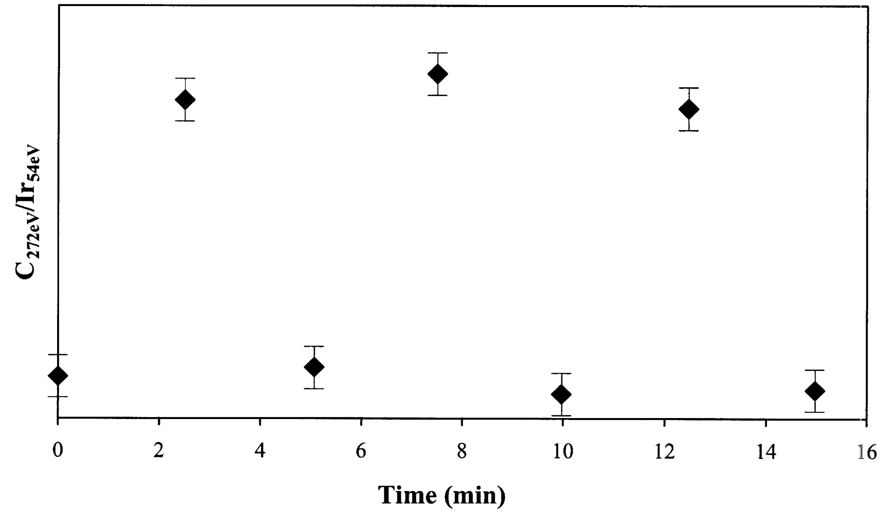

Figure 8. The variation of the $C_{272\,eV\,(of\,adsorbed\,CO)}/Ir_{54\,eV}$ AES signal ratio at 460 K during rate oscillations (N_2O pressure of 1×10^{-6} mbar and CO/N_2O ratio of 0.11). Error bars are shown.

form of water [5]. These observations suggest that the mechanism of oscillatory behavior is different for the two reactions, due to the inhibitive effect of the reducing gas in the N_2O–CO reaction on the N_2O dissociation. For the N_2O–H_2 reaction it is only a high concentration of O_{ads} that inhibits N_2O decomposition. For the N_2O–CO reaction such an oscillation in O_{ads} concentration was not found. Here the CO_{ads} concentration shows oscillatory behavior that masks the expected oscillation in O_{ads} concentration.

This mechanism explains the counter-phase relationship found between oscillations for N_2O and N_2 pressures, and those of CO and CO_2. It also considers the inhibition of N_2O decomposition caused by CO and the described periodic transitions between a CO-rich (inactive) and a CO-poor (active) surface. The low CO-coverage would then correspond to the maxima of N_2O decomposition, that is, the maximum of N_2 and minimum of N_2O pressures, during the oscillations.

The purpose of this short discussion was to invoke several possible steps that may be relevant for the mechanism of oscillations in the N_2O–CO and N_2O–H_2 reactions. Detailed studies, both experimental and modeling, are needed for a complete understanding of the oscillatory behavior of N_2O reduction.

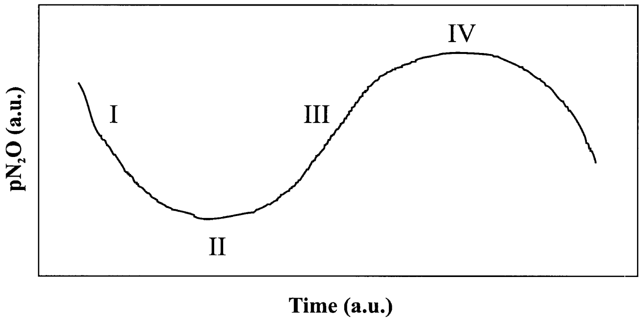

Figure 9. Specific form of an oscillation cycle for the N_2O–CO reaction (possible mechanism discussed in the text).

Interestingly, these results show that the pressure of the reactant N_2O oscillates in an almost counter-phase with that of the other reactant CO. To the best of our knowledge, this is the first time that a counter-phase relationship has been reported for rate oscillations in the reactant pressures. More research needs to be done to further clarify this phenomenon.

The N_2O conversion was less than 7% during the oscillations. Most probably, rate oscillations for CO/N_2O reaction are only possible in large excess of N_2O. This is due to combined effects of the high sticking probability of CO at these low temperatures, the relatively low sticking probability of N_2O (even on CO free surfaces), and the large inhibitive effect of CO_{ads} on N_2O dissociation. The oscillations then occur only for very low CO/N_2O ratios and very low values of temperature, which is in contrast to the N_2O–H_2 reaction that had no inhibition by H_2. In this case, the ratios where oscillations were observed were close to unity [5].

The rate oscillations of the N_2O–CO reaction are also very sensitive to changes in the CO/N_2O ratio or temperature like those reported for the N_2O–H_2 reaction on the same surface [5]. Therefore the rate oscillations could not be followed for extended periods of time (maximum of 45 min), because of small uncontrolled changes in the partial pressures. However, in principle, the oscillations are sustained. For temperatures just out of the aforementioned range, small instabilities in the rate were observed. These processes were found to be triggered by small variations in temperature, like those reported previously for the N_2O–H_2 reaction on the same surface [5].

4. Conclusions

The reaction with H_2 is faster for temperatures up to 550 K (depending on the N_2O/reducing gas ratio), due to CO inhibition of the decomposition of N_2O. Oscillations in rate were found between 373 and 377 K, for very low CO/N_2O ratios (close to 0.1). The reaction products were N_2 and CO_2. N_2 oscillates in anti-phase with reactant N_2O and CO in anti-phase with CO_2. Synchronous events, highly correlated in time, were found for all masses in regular time intervals. A possible explanation for the oscillations is proposed, based on periodic transitions between a CO-rich (inactive) and a CO-poor (active) surface. In contrast, the rate oscillations for the N_2O–H_2 reaction are related to periodic transitions between O-rich and O-poor surfaces.

Acknowledgments

This work has been performed under the auspices of NIOK, The Netherlands Institute for Catalysis Research, laboratory report UL 01-2-03, and of NRSC-Catalysis. The project was supported by the NRSC-Catalysis and partly by INTAS (99#-01882).

References

[1] J.N. Armor, Appl. Catal. B: Env. 1 (1992) 221.
[2] F. Kapteijn, J. Rodriguez-Mirasol and J.A. Moulijn, Appl. Catal. B: Env. 9 (1996) 25.
[3] G. Centi, L. Dall'Olio and S. Perathoner, J. Catal. 192 (2000) 224.
[4] G. Centi, L. Dall'Olio and S. Perathoner, J. Catal. 194 (2000) 130.
[5] S.A. Carabineiro and B.E. Nieuwenhuys, Surf. Sci. 495 (2001) 1.
[6] R.W. McCabe and C. Wong, J. Catal. 121 (1990) 422.
[7] R.R. Sadhankar, J. Ye and D. Lynch, J. Catal. 146 (1994) 511.
[8] B. Cho, J. Catal. 148 (1994) 697 and references therein.
[9] R.R. Sadhankar and D. Lynch, J. Catal. 149 (1994) 278.
[10] J.H. Holles, M.A. Switzer and R.J. Davis, J. Catal. 190 (2000) 247.
[11] B.E. Nieuwenhuys and G.A. Somorjai, Surf. Sci. 72 (1978) 8.
[12] B.E. Nieuwenhuys, *Elementary Reaction Steps in Heterogeneous Catalysis*, ed. R.W. Joyner and R.A. van Santen (Kluwer, Dordrecht, 1993), p. 155.
[13] G. Ertl, Adv. Catal. 37 (1992) 213.
[14] B.E. Nieuwenhuys, Surf. Sci. 126 (1983) 307
[15] B.E. Nieuwenhuys, Adv. Catal. 44 (1999) 259.
[16] C.A. de Wolf, B.E. Nieuwenhuys, M.M. Slinko and M.Yu Smirnov, Surf. Sci. 433–435 (1999) 63.
[17] P.D. Cobden, C.A. de Wolf, M.Yu. Smirnov, A. Makeev and B.E. Nieuwenhuys, J. Molec. Catal. A: Chem. 158 (2000) 115.
[18] Y. Matsumoto, J. Lee, H. Kato and K. Sawabe, *Proc. SPIE—The International Society for Optical Engineering*, vol. 2125, *Laser Techniques for Surface Science*, ed. H.-L. Dai and S.J. Sibener (1994) p. 303.
[19] Y. Li and M. Bowker, Surf. Sci. 348 (1996) 67.
[20] S. Haq and A. Hodgson, Surf. Sci. 463 (2000) 1.